Modified Degree of Polarization Function for Rough Metallic Surface Parameter Estimation Based on Multispectral Polarimetric Measurement

XIN WANG[1,2], JING YUAN[1,2], CHANGXIANG YAN[1,3], YANFENG QIAO[1], JUNQIANG ZHANG[1], XUEPING JU[1], NING DING[1,2], AND YOUZHI DONG[1,2]

[1]Changchun Institute of Optics, Fine Mechanics and Physics, Chinese Academy of Sciences, Changchun 130033, China
[2]University of Chinese Academy of Sciences, Beijing 100049, China
[3]Center of Materials Science and Optoelectrics Engineering, University of Chinese Academy of Science, Beijing 100049, China

Corresponding author: Changxiang Yan (yancx@ciomp.ac.cn)

ABSTRACT In order to recognize different materials from passive polarimetric measurements specifically, a model that can describe the distribution of polarization energy scattered from the target surface is needed for estimating the parameters of interest (complex refractive index n, k and surface roughness σ) of targets. This paper presents a new method for targets parameters estimation. The presented method modifies the degree of linear polarization (DOLP) model by introducing the Lorentz-Drude dispersion constants which do not vary with wavelength as well as the diffuse component of reflection related to the surface roughness to the DOLP equation. This solves the problem of difficulty and inaccuracy caused by multi-angle passive polarimetric measurements used by previous works and helps to improving the parameters estimation accuracy for rough targets. The Monte Carlo simulations result illustrate that the presented method is robust to Gaussian noise. Moreover, the experimental results of rough aluminium plate and rough copper plate validate the effectiveness of the presented model. The errors of estimated n are about 8% for aluminium plate and 9% for copper plate. The errors of estimated k are less than 4% for aluminium plate and no more than 5% for copper plate. The errors of estimated surface roughness σ are about 6.8% and about 6% for aluminium plate and copper plate respectively. The high estimation accuracy and less detection angle requirement achieved by the presented method are significant for material characterization in passive remote sensing application.

INDEX TERMS Polarization, refractive index estimation, degree of linear polarization, surface roughness, remote sensing recognition, Lorentz-Drude model.

I. INTRODUCTION

Polarization is a property of light complementing other electromagnetic radiation attributes such as intensity, frequency, or spectral characteristics [1], [2]. Different characteristics of object such as surface roughness and complex refractive index will change the polarization state of light that reflected from the object surface in varying ways [3]–[6]. In this case, there are obvious differences in polarization information between different targets on account of the greatly distinction in their surface characteristics and internal composition. This makes passive-polarization-based remote sensing applicable for many applications including targets recognition [7]–[11] and material classification [12], [13].

Early work on the utility of passive polarimetry for remote sensing applications was published by Thilak *et al.* [14]. They presented a method to estimate the complex index of refraction of specular targets from multiple-angle polarimeter

The associate editor coordinating the review of this manuscript and approving it for publication was Jon Atli Benediktsson.

measurements. They contributed to developing an effective algorithm based on DOLP model and nonlinear least-squares estimation. Their method is robust to the reflection angle. However, they did not take into account the law that complex refractive index changes with the wavelength. As a result, these models can only use multi-angle polarization information to estimate the complex refractive index. Besides, their methods cannot analyze the surface characters of targets.

Hyde *et al.* [15] proposed a method to estimate the complex index of refraction of an unknown object from multiple-angle polarimeter measurements. In order to improve the estimating accuracy, they developed a blind-deconvolution algorithm to correct measured degree of linear polarization (DOLP) until it fits the DOLP priors. And they took diffuse reflection into account in the DOLP expression. Their method is advantaged to improve the estimating accuracy of the surface parameters of unknown object. However, they also neglected the fact that complex refractive index changes with the wavelength. This limits the applicability of their methods since multi-angle polarization detection would result in the inaccuracy and difficulty in remote sensing applications. Besides, their method depends on the prior values.

Sawyer *et al.* [16] presented a method for characterization of unknown specular targets using passive multispectral polarimetric imagery. They substituted the refractive index n and k in DOLP expression with the Drude dispersion constants, which makes their method able to estimate the complex refractive index of specular targets from multispectral polarimetric measurements. However, they ignored the diffuse component of reflection which leads to the impact of lowering the DOLP value, reducing the estimation accuracy of complex refractive index for roughened targets.

Yang *et al.* [17] presented a method to estimate refractive index and surface roughness simultaneously from both multispectral and multiangular passive polarimetric measurements. Their method is advantaged to impose more constrains in their estimation algorithm to improve the estimate results. However, the Drude model is not suitable for describing the dispersion characteristics of metallic materials near their absorption band, which limits the estimation accuracy.

To solve these problems, this paper presents a new method to estimate the material parameters of rough targets based on the modified DOLP equation. In order to make full use of the multispectral polarimetric measurements, we introduce Lorentz-Drude dispersion constants [18] which do not vary with wavelength to the expression of DOLP. This makes the presented method applicable to estimating the material parameters of roughened targets from multispectral polarimetric measurements without changing angles, which contributes to avoiding the image shift between the collected multi-angle passive polarimetric remote sensing images. Besides, Lorentz-Drude model is widely used for describing the dispersion characteristics of metallic material and is effective over their absorption band, which makes Lorentz-Drude model more applicable than Drude model [19]. In addition, the diffuse component of reflection which is sensitive to the

surface roughness is helpful to describe the polarization state of scattering light more accurate, which reducing the impact of surface status to the refractive index estimation [17]. Therefore, taking the diffuse component of reflection into consideration makes the presented method more appropriate for rough targets. Then, based on the modified DOLP equation, the complex refractive index and surface roughness can be accurately estimated from multispectral polarimetric measurements using a nonlinear least-squares estimation algorithm.

The paper is organized as follows: Section II derives and modified the expression for the degree of linear polarization (DOLP) based on pBRDF model and Lorentz-Drude model, and describes the estimation method. Section III analyzes the sensitivity of presented method to the number of input measurements and Gaussian noises by Monte Carlo simulations. Section IV analyzes the experimental results to validate our method. Section V presents the conclusion.

II. THEORY
A. PBRDF MODEL
The polarization state of light would change when scattered from target surface, which can be formulated by the polarization bidirectional reflection distribution function (pBRDF) [20]. This function could characterize the polarization state of both specular component and diffuse component of scattered light for a wide variety of materials. We present the pBRDF equations necessary for our work here to derive the DOLP expression. The geometry that specifies the pBRDF is illustrated in Fig. 1.
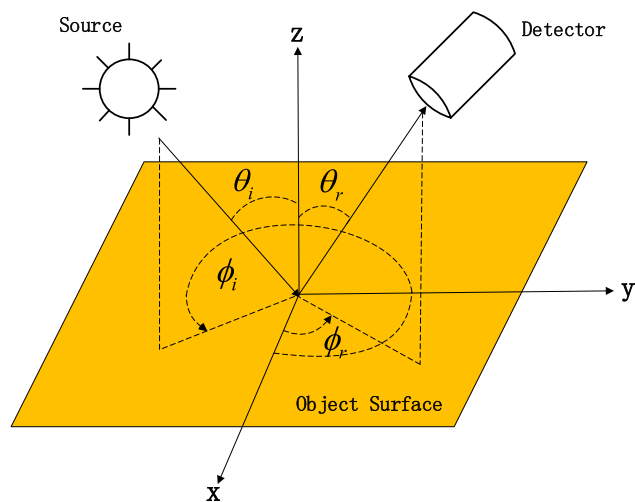
FIGURE 1. Measurement geometry of presented method where θ_i and θ_r are the incident zenith and reflected zenith angles, ϕ_i and ϕ_r are the incident azimuth and reflected azimuth angles respectively.

The pBRDF Mueller matrix f describes the relationship between inputted Stokes vector S_i and observed Stokes vector S_r. These vectors are related to the polarization

characteristic of light [21].

$$\begin{bmatrix} S_0^r \\ S_1^r \\ S_2^r \end{bmatrix} = f \bullet \begin{bmatrix} S_0^i \\ S_1^i \\ S_2^i \end{bmatrix} = \begin{bmatrix} f_{00} & f_{01} & f_{02} \\ f_{10} & f_{11} & f_{12} \\ f_{20} & f_{21} & f_{22} \end{bmatrix} \bullet \begin{bmatrix} S_0^i \\ S_1^i \\ S_2^i \end{bmatrix} \quad (1)$$

The inputted Stokes vector S_i is concerned with the polarization information of incident light. The observed Stokes vector S_r denotes the polarization information of reflected light which can be measured by polarimeter. The following drops the element in the i_{th} row and j_{th} column of pBRDF Mueller matrix, f_{ij} for clarity.

pBRDF Mueller matrix f is consisted of the specular component f^s and diffuse component f^d [22]

$$f = f^s + f^d \quad (2)$$

The specular component f^s is derived using the microfacet surface model [23]. According to the microfacet surface model, a rough surface is regarded as a collection of randomly oriented facets with Gaussian distribution. Each individual microfacet is assumed to be a specular reflector obeying Fresnel's equation. With these assumptions, i_{th} row and j_{th} column of the pBRDF Mueller matrix f_{ij}^s can be expressed as:

$$f_{ij}^s(\theta_i, \theta_r, \Delta\phi, n, k, \sigma)$$
$$= \frac{\exp[\frac{-(\tan\theta)^2}{2\sigma^2}]}{8\pi\sigma^2\cos\theta_r\cos\theta_i(\cos\theta)^4}$$
$$\times G(\theta_i, \theta_r, \phi) \times \mathbf{M_{ij}}(\theta_i, \theta_r, \Delta\phi, n, k) \quad (3)$$

where θ_i and θ_r denote the incident zenith angle and reflected zenith angle with respect to the surface normal $\vec{z}$. n and k are refractive index and extinction coefficient which represent the real part and imaginary part of complex refractive index respectively. $\Delta\phi = \phi_i - \phi_r$, where ϕ_i and ϕ_r denote the incident azimuth and reflected azimuth angles, σ is the surface roughness, which is equivalent to the standard deviation of the surface slope. $\mathbf{M_{ij}}$ denotes the element in the i_{th} row and j_{th} column of the Fresnel reflectance Mueller matrix, θ is the angle between the surface normal of a microfacet and the mean surface normal:

$$\theta = \arccos\left(\frac{\cos\theta_i + \cos\theta_r}{2\cos\beta}\right) \quad (4)$$

β represents the angle between the surface normal of a microfacet and the incident light.

$$\beta = \frac{1}{2}\arccos(\cos\theta_i\cos\theta_r + \sin\theta_i\sin\theta_r\cos\Delta\phi) \quad (5)$$

G is the visibility function, which describes the shadowing factor of microfacet [22].

$$G(\theta_i, \theta_r, \Delta\phi) = \min(1; \frac{2\cos\theta_i\cos\theta}{\cos\beta}; \frac{2\cos\theta_r\cos\theta}{\cos\beta}) \quad (6)$$

The diffuse component f^d derived with the directional hemispherical reflectance ρ_{DHR} [22] usually exists in the

first row and first column of pBRDF Mueller matrix can be expressed as:

$$f_{00}^d(\theta_i, \sigma) = \frac{[1 - \rho_{DHR}(\theta_i, \sigma)]}{\pi} \quad (7)$$

$$\rho_{DHR} = \int_0^{2\pi}\int_0^{\frac{\pi}{2}} f_{00}^s\cos\theta_r\sin\theta_r d\theta_r d\varphi \quad (8)$$

ρ_{DHR} denotes the hemispheric directional reflection integral function describing the distribution of scattered light in the hemispheric space of object surface.

Based on the derivation above, the full pBRDF expression f can be obtained by combining the specular component f^s with the diffuse component f^d, where the first element f_{00} represents the total intensity of the reflected light (the sum of the intensity of the specular and diffuse reflections). The remaining elements f_{ij} represent the intensity of the light at different polarization components where $i, j \neq 0$.

$$f_{00}(\theta_i, \theta_r, \phi, n, k, \sigma) = f_{00}^s(\theta_i, \theta_r, \phi, n, k, \sigma)$$
$$+ \frac{[1 - \rho_{HDR}^{s,PEC}(\theta_i, \sigma)]}{\pi} \quad (9)$$
$$f_{ij}(\theta_i, \theta_r, \phi, n, k, \sigma) = f_{ij}^s(\theta_i, \theta_r, \phi, n, k, \sigma) \quad (10)$$

B. DERIVATION AND MODIFICATION OF THE DEGREE OF POLARIZATION

This paper assumes that the illumination source is unpolarized, which is the case in passive remote sensing applications, and the measurements are performed for the case of scattering in the plane of incidence, where $\Delta\phi = \pi$. With these assumptions, the Stokes vector of illumination source in (11) is given by $\mathbf{S_{0i}} = \begin{bmatrix} 1 & 0 & 0 \end{bmatrix}^T$, θ and β can be simplified as $\theta = \frac{1}{2}(\theta_i - \theta_r)$, $\beta = \frac{1}{2}(\beta_i + \beta_r)$, then the Stokes vector of reflected light is given by:

$$\begin{bmatrix} S_0^r \\ S_1^r \\ S_2^r \end{bmatrix} = \begin{bmatrix} f_{00} & f_{01} & 0 \\ f_{10} & f_{11} & 0 \\ 0 & 0 & f_{22} \end{bmatrix} \bullet \begin{bmatrix} 1 \\ 0 \\ 0 \end{bmatrix} = \begin{bmatrix} f_{00} \\ f_{01} \\ 0 \end{bmatrix} \quad (11)$$

The degree of linear polarization (DOLP) of reflected light can be expressed in terms of the Stokes parameters as:

$$P = \frac{\sqrt{S_1^{r2} + S_2^{r2}}}{S_0^r} \quad (12)$$

Combining (3), (11), (12), the DOLP equation which contains the diffuse component of pBRDF model is derived from the pBRDF model [15] as:

$$P = \frac{f_{10}^s}{f_{00}^s + f_{00}^d} = \frac{2A\sin^2\beta\cos^2\beta}{A^2\cos^2\beta + \sin^4\beta + B^2\cos^2\beta}$$
$$\times \frac{\Gamma}{\Gamma + (1 - \int_0^{2\pi}\int_0^{\frac{\pi}{2}} f_{00}^{s,PEC}\cos\theta_i\sin\theta_r d\theta_r d\phi)/\pi}$$
$$(13)$$

$$\Gamma = \frac{G(\theta_i, \theta_r, \Delta\phi)\exp[-\frac{\tan\theta^2}{2\sigma^2}]}{8\pi\sigma^2\cos\theta_i\cos\theta_r\cos^4\theta} \quad (14)$$

$$A = \sqrt{\frac{\sqrt{C} + D}{2}} \qquad (15)$$

$$B = \sqrt{\frac{\sqrt{C} - D}{2}} \qquad (16)$$

$$C = 4n^2k^2 + D^2 \qquad (17)$$

$$D = n^2 - k^2 - \sin^2 \beta \qquad (18)$$

In order to present an applicable equation to estimate the n and k of rough targets from multispectral polarimetric measurements, the DOLP equation should not contains variables that vary with wavelength. However, the n and k of metallic materials in the pBRDF based DOLP equation are sensitive to wavelength. Therefore, an innovated DOLP equation was formed by substituting the Lorentz-Drude dispersion constants which do not vary with wavelength in place of n and k in the DOLP equation.

Lorentz-Drude model is applicable for describing the relationship between dielectric constant ($\varepsilon = \varepsilon_r - i\varepsilon_i$) and dispersion constants of metallic materials over wide spectral range. The refractive index n, k are defined as the square root of the complex relative dielectric constant ($\varepsilon_r = n^2 - k^2$, $\varepsilon_i = 2nk$). Therefore, Lorentz-Drude model could relate n, k to the dispersion constants as:

$$n^2 - k^2 = \varepsilon_r = 1 - \frac{f_0 \omega_p^2}{\omega^2 + \gamma_0^2} + \sum_{i=1}^{3} \frac{f_i \omega_p^2 (\omega_i^2 - \omega^2)}{(\omega_i^2 - \omega^2)^2 + \gamma_i^2 \omega^2} \qquad (19)$$

$$2nk = \varepsilon_i = \frac{f_0 \omega_p^2 \gamma_0}{\omega^3 + \gamma_0^2 \omega} + \sum_{i=1}^{3} \frac{f_i \omega_p^2 \gamma_i \omega}{(\omega_i^2 - \omega^2)^2 + \gamma_i^2 \omega^2} \qquad (20)$$

where $\omega = \frac{2\pi c}{\lambda}$, ω_p is plasma frequency, γ_0 is electron relaxation rate, ω_i is oscillators frequency, γ_i is oscillators relaxation rate and f_i is oscillators strength. These parameters are Lorentz-Drude dispersion constants which can be regarded as constants that independent to wavelength for metals.

Then, using Lorentz-Drude dispersion constants to substitute n and k, C and D in (17), (18) can be expressed as:

$$C = \left(\frac{f_0 \omega_p^2 \gamma_0}{\omega^3 + \gamma_0^2 \omega} + \sum_{i=1}^{3} \frac{f_i \omega_p^2 \gamma_i \omega}{(\omega_i^2 - \omega^2)^2 + \gamma_i^2 \omega^2} \right)^2$$
$$+ \left(1 - \frac{f_0 \omega_p^2}{\omega^2 + \gamma_0^2} + \sum_{i=1}^{3} \frac{f_i \omega_p^2 (\omega_i^2 - \omega^2)}{(\omega_i^2 - \omega^2)^2 + \gamma_i^2 \omega^2} - \sin^2 \beta \right)^2 \qquad (21)$$

$$D = 1 - \frac{f_0 \omega_p^2}{\omega^2 + \gamma_0^2} + \sum_{i=1}^{3} \frac{f_i \omega_p^2 (\omega_i^2 - \omega^2)}{(\omega_i^2 - \omega^2)^2 + \gamma_i^2 \omega^2} - \sin^2 \beta \qquad (22)$$

The modified DOLP equation used for estimation is finally derived by combining (13), (21) and (22).

C. ESTIMATION OF n k AND σ

In order to estimate the complex refractive index from multispectral polarimetric measurements, the DOLP equation in

this paper breaks the n and k into Lorentz-Drude dispersion constants which do not vary with wavelength. Therefore, based on the modified DOLP equation, the dispersion constants and surface roughness are inversed from the multispectral DOLP measurements first using nonlinear least-squares algorithm, which is expressed as:

$$e^2 = \frac{1}{N} \sum_{k=1}^{N} [P_t(\theta_i, \theta_r, \lambda_k, \sigma, d) - P_m(\theta_i, \theta_r, \lambda_k)]^2 \qquad (23)$$

P_t is modified DOLP equation, which denotes the theoretical DOLP value. d is dispersion constants in (19), (20). P_m is measured DOLP value. θ_i is incident angle, θ_r is detection angle, σ is surface roughness. λ_k denotes the specific spectral channel and N is the number of spectral channels for measurements.

We see the modified DOLP equation P_t is a function related to, θ_i, θ_r dispersion constants d, σ and λ. So, based on the modified DOLP equation and measured multispectral DOLP value P_m with known θ_i, θ_r and λ, the surface roughness σ and dispersion constants d could be inversed when they satisfy the measured DOLP values of N spectral channels and minimize the square deviation e between P_t and P_m.

The refractive index n, k are functions related to dispersion constants d, and λ. So, after getting the estimated dispersion constants d, the n, k of each wavelength could be estimated by putting the inversed dispersion constants d to (24), (25) to calculate the n, k at specific wavelength λ_k.

$$n(\lambda_k) = \sqrt{\frac{\sqrt{\varepsilon_i^2 + \varepsilon_r^2} + \varepsilon_r}{2}} \qquad (24)$$

$$k(\lambda_k) = \sqrt{\frac{\sqrt{\varepsilon_i^2 + \varepsilon_r^2} - \varepsilon_r}{2}} \qquad (25)$$

III. SIMULATION

In order to validate the presented method for parameters estimation from noisy inputs, this section analyzes the sensitivity of the proposed method to the number of input measurements as well as different levels of Gaussian noises from 1000 Monte Carlo simulation trials [24]. The simulation results are evaluated by the standard deviation (STD) as well as root-mean-square error (RMSE), which indicates the discrete degree of data set and the deviation between the observed value and true value respectively.

$$STD = \sqrt{\frac{1}{N} \sum_{i=1}^{N} (e_i - \bar{e})^2} \qquad (26)$$

$$RMSE = \sqrt{\frac{1}{N} \sum_{i=1}^{N} (e_i - r_i)^2} \qquad (27)$$

e_i denotes the estimated value, r_i denotes the reference value and $\bar{e}$ denotes the mean of estimated value.

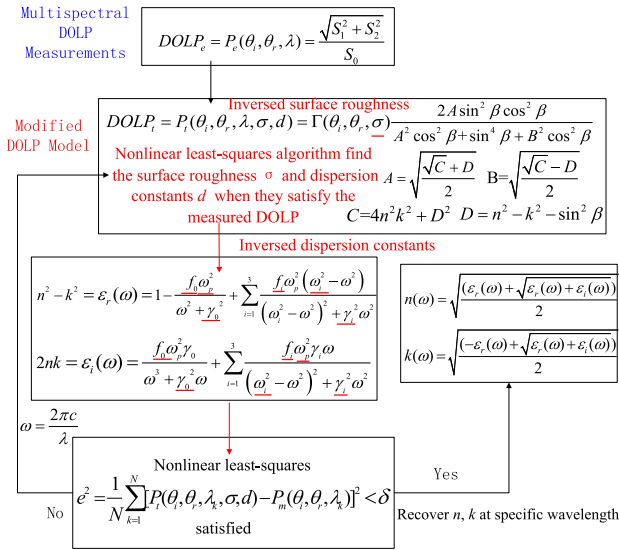Synthetic data for simulations are given by the DOLP expression in Eq. (13), with specific input values for σ, θ_i, θ_r,

FIGURE 2. Parameters estimation algorithm flow chart.

TABLE 1. Input dispersion constants for simulation [18].

Input parameters	Value
ω_P	1.64×10^{16} rad/s
ω_1	4.14×10^{14} rad/s
ω_2	4.48×10^{15} rad/s
ω_3	8.04×10^{15} rad/s
γ_0	4.6×10^{-14} rad/s
γ_1	5.73×10^{-16} rad/s
γ_2	1.6×10^{-15} rad/s
γ_3	4.87×10^{-15} rad/s
f_0	0.575
f_1	0.061
f_2	0.104
f_3	0.723

TABLE 2. Simulation results for 0.1% Gaussian noise.

spectral channels	n	k	σ
16	0.3012±0.0155	3.7184±0.0557	0.3491±0.0701
21	0.3084±0.0138	3.7422±0.0493	0.3560±0.0497
26	0.3102±0.0130	3.7447±0.0471	0.3657±0.0433
31	0.3080±0.0129	3.7440±0.0467	0.3663±0.0410
34	0.3077±0.0130	3.7444±0.0464	0.3671±0.0477

TABLE 3. Simulation results for 2% Gaussian noise.

spectral channels	n	k	σ
16	0.2955±0.0463	3.8861±0.3356	0.3344±0.1199
21	0.2977±0.0230	3.8316±0.1140	0.3419±0.0706
26	0.2981±0.0217	3.8276±0.1327	0. 3471±0.0749
31	0.2988±0.0192	3.8246±0.1311	0.3491±0.0744
34	0.2990±0.0193	3.8180±0.1239	0.3493±0.0702

dispersion constants, and a sequence of numbers for spectral channels. The surface roughness σ is equal to 0.37 to be the same as the surface roughness of our experiment samples. The θ_i and θ_r are fixed at 45° because it is within the specular lobe of the samples [14] and the signal is strong in this area. In order to analyze the sensitivity of presented method to different numbers of input measurements, the λ ranges from 450nm to 750 nm with various step size values of 20nm, 15nm, 12nm, 10nm and 8nm to obtain spectral channels of 16, 21, 26, 31 and 36 respectively in different simulations. We choose this detection spectral range because the signal of our experiment instrument here is much larger than the noise and the polarization effect of the experiment instrument itself over 450-750nm is negligible [25].

The synthetic data sets are then added with white Gaussian noises in order to analyze the robustness of the proposed method to the noisy inputs. The standard deviations of Gaussian noises are equal to 0.1% and 2% of the synthetic DOLP values to simulate different levels of noisy DOLP measurements. Then, the noisy synthetic data sets are input to the Levenberg–Marquardt solver for estimation. The dispersion constants and surface roughness σ are returned by the solver first and the complex refractive index n, k are then calculated from the Lorentz-Drude model at specific wavelengths. The estimation method and the whole estimation process are described in details in figure 2.

Table 2, Table 3 and Fig. 3 show the Monte Carlo simulation results of two different Gaussian noise scenarios. The input parameters of sample are assumed to be copper with the complex refraction index given by $n = 0.309$, $k = 3.75$ at 650 nm and surface roughness σ of 0.37. From Table 2 we observe that in the low-noise case, the estimated results for refractive index and surface roughness are consistent well with the input values and the RMSE plots in Figure 3 show

a slight improvement in estimate accuracy when the number of spectral channels increases from 16 to 21 while no more obvious improvement appears beyond 21. This phenomenon is more apparently observed in high-noise case. Due to the noise level, the estimated results of high-noise case in Table 3 deviate a bit from the input values, however, the estimated result again improved with increasing number of spectral, which is clear from a dramatic reduction in RMSE and the average values that become more accordant with the input values, from 16 to 21, while the RMSE plots indicate that no further improvement in the accuracy of the estimates appears beyond 21 spectral channels. We could see the RMSE of high-noise case has a slightly increasing trend as the spectral channels rising from 26 to 34 in figure 3(a) and 3(c). This
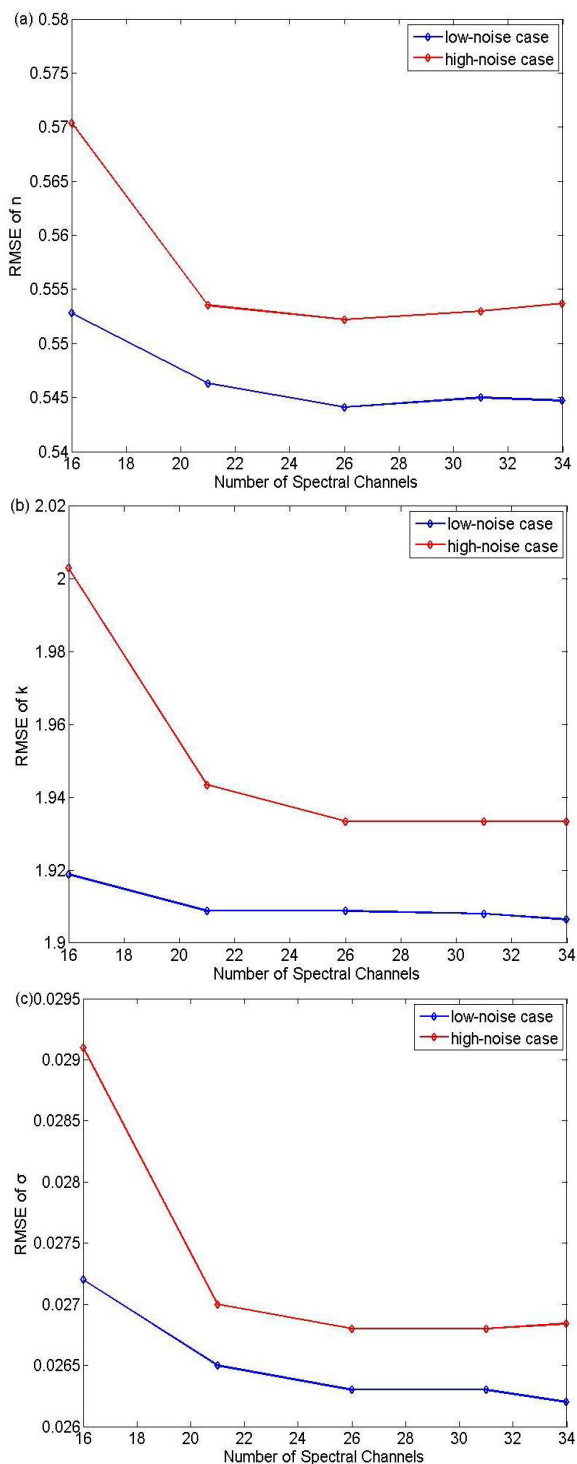
FIGURE 3. Simulation results of RMSE related to Number of spectral channels for copper at 650 nm in low-noise case and high-noise case. (a) the RMSE of the refractive index *n*; (b) the RMSE of the extinction coefficient *k*; (c) the RMSE of the surface roughness σ. The reference indices of copper are $n = 0.309$, $k = 3.75$ at 650 nm and $\sigma = 0.37$. The results are achieved from 1000 Monte Carlo trials.

is because the number of spectral channels for estimation reaches saturation point at 16, at the same time, the algorithm converges. Therefore, the RMSE may have a reasonably slight fluctuation even increase a bit.

The Monte Carlo simulation results indicates that the estimation accuracy of the presented method improves with an increasing number of spectral channels until saturated. Besides, the estimation accuracy of the presented method depends on the level of measurement noise. In the low-noise case, the complex refraction index and surface roughness are estimated to a high degree of accuracy and the saturation number of spectral channels for accurate estimation is 21. In the high-noise case which is consistent with the measure accuracy of our experiment instruments, the accurate estimation for the complex refraction index and surface roughness is reasonably more difficult than low-noise case. However, the estimated results accordant well with the input values when the number of spectral channels reaches saturation point of 21. Therefore, we denote that the refractive index and surface roughness can be retrieved from noisy simulated data by the method we present.

We mention that in order to estimate the complex refraction index of metallic material accurately from multispectral polarimetric measurements, the presented method employs an appropriate dispersion model that contains a plenty of constants, therefore at least 13 spectral polarimetric measurements are needed to put into the algorithm in the process of estimation. However, this does not limit effectiveness of the presented method in passive remote sensing application since obtaining a plenty of multispectral polarimetric measurements is not a tough task with the development of multispectral detection technique [26]. The spectroradiometer used in the following experiment has a spectral resolution of 1 nm and spectral range from 350nm to 2500nm, which is applicable for data collection. Besides, compared with previous methods that depend on multi-angle measurements for estimation [14], [15], the presented method is helpful for avoiding the direction measurement error caused by changing angles in experiment analysis and the image shift brought by multi-angle polarization imaging in passive remote sensing application.

IV. EXPERIMENT

The DOLP of the reflected light is collected with the Northeast Normal University Laboratory Goniospectrometer System (NENULGS) in our experiment. As shown in Fig. 4. The NENULGS consists of a tungsten halogen lamp, a goniometer and an Analytical Spectral Devices Field-Spec 3 (ASD FS3) spectroradiometer. The tungsten halogen lamp is used as the source of unpolarized illumination which is attached to a 90° arc with a 1.5 m radius from the sample holder. The goniometer is used to perform measurements with zenith angles ranging from −90° to 90° and azimuth angles ranging from 0° to 360°. The ASD FS3 spectroradiometer is utilized to obtain spectral polarized reflectance. To measure the radiance in different polarization directions, a calcite Glan-Thomson prism, which allows for rotation from 0° to 360° in 1° increments, is used in front of the fiber-optic detector of the spectroradiometer and the spectral resolution
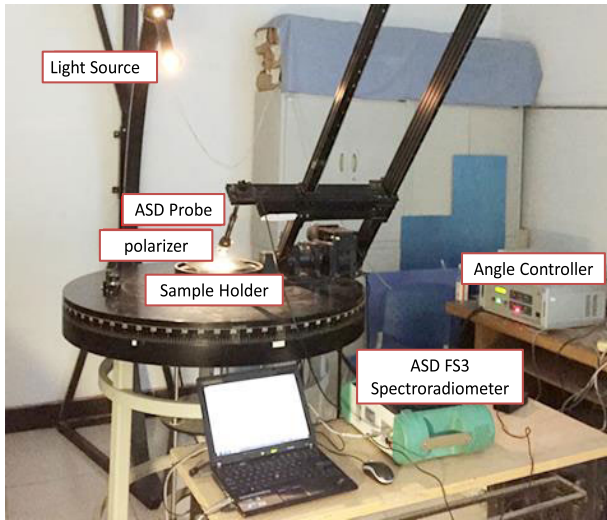
FIGURE 4. The equipment drawing of DOLP measurement for specimen.

FIGURE 5. Measured and estimated DOLP plots for copper plate. The illuminate angle and detection angle are fixed at 45°.

FIGURE 6. Measured and estimated DOLP plots for aluminium plate. The illuminate angle and detection angle are fixed at 45°.

of our ASD FS3 spectroradiometer is 1 nm. More details about the NENULGS can be found in Ref [27].

The surface roughness is measured by Taylor Hobson PGI-830 surface profiler which has a resolution of 0.8 nm and the measurements generated a data set of 50,000 surface points for each sample. The standard deviation of surface slope σ in radians is then derived from the measured rootmean-square (rms) roughness in meters and surface correlation lengths of the samples.

According to Rayleigh criterion: when the phase difference of two rays on a rough surface is greater than $\pi/2$, that is, if $\delta > \lambda/8\cos\theta_i$, the surface is defined as a rough surface, where δ is rms roughness, θ_i is incident angle otherwise, it is a smooth surface. In this paper, the root-mean-square height of copper and aluminum are $1.43\mu m$ and $1.32\mu m$ respectively, and the incidence angle is 45°, which conforms to Rayleigh criterion and applies to the previous theoretical derivation.

The target samples in our experiments are roughened aluminium plate and roughened copper plate. They are mounted on the sample holder which is at the rotation center of the detector and source. The samples are leveled using a bubble leveler so that the experiment circumstance is consistent with the observation geometry of the theoretical model.

The incident zenith angle θ_i, and detection zenith angle θ_r are fixed at 45°, 50°, 55°, the relative azimuth angle $\Delta\phi$ is fixed at 180° for this region is a relatively bright area of reflection centered and the detected signal is high. Besides, we take the average of ten sets of measurements during collecting data to reduce the noise. The selected detection spectral band ranges from 450nm to 750nm where the polarization disturb of the experiment instrument itself is negligible and the signal is much larger than the noise.

The measured DOLP can be derived from the Stokes vector of reflected light as expressed in (24) [28].

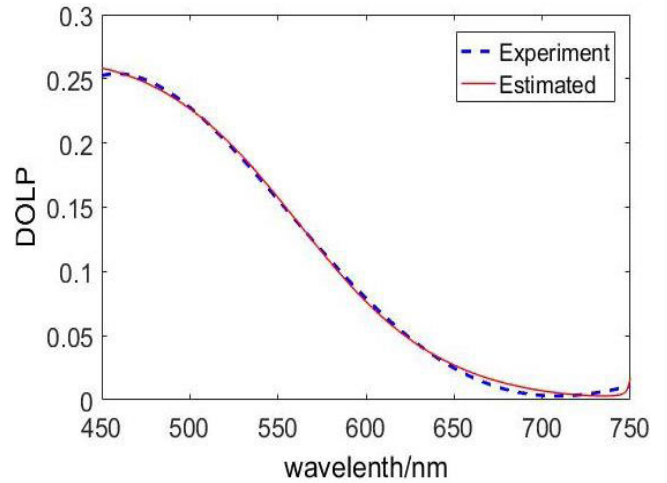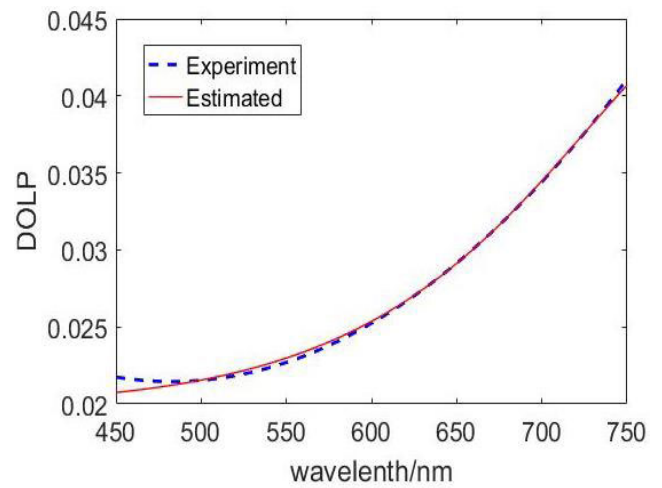$$P = \sqrt{\frac{Q^2 + U^2}{I}} \qquad (28)$$

where I, Q, and U are the first three column of Stokes vector of reflected light: $\mathbf{S} = \begin{bmatrix} I & Q & U \end{bmatrix}^T$. The expressions for I, Q, and U are given by.

$$I = I_0 + I_{90} = I_{45} + I_{135} \qquad (29)$$
$$Q = I_0 - I_{90} \qquad (30)$$
$$U = I_{45} - I_{135} \qquad (31)$$

I_0, I_{45}, I_{90} and I_{135} are the light intensities measured with the analyzer oriented at 0°, 45°, 90°, and 135° respectively.

Fig. 5 and Fig. 6 show the measured DOLP values and estimated DOLP values for aluminium plate and copper plate. The illuminate angle θ_i and detection angle θ_r are fixed at 45°, the relative azimuth angle $\Delta\phi$ is fixed at 180° and spectral ranges from 450nm to 750 nm with step size of 1 nm. We observe that the estimated DOLP plots consistent well with the measured DOLP plots in every spectra channel, which validates the effectiveness of our method for metallic materials refractive index estimation. We mention that

TABLE 4. Estimated complex refractive index and percent error of copper plate at 45° [29], [31].

Wavelength(nm)	450	550	650	750
Estimated *n*	1.18	0.53	0.27	0.25
Reference *n*	1.16	0.79	0.22	0.23
Error (%) *n*	2.00	32	22	9.5
Estimated *k*	2.30	2.85	3.76	4.42
Reference *k*	2.40	2.6	3.67	4.61
Error (%) *k*	4.17	9.70	2.40	4.10

TABLE 5. Estimated complex refractive index and percent error of aluminium plate at 45° [30].

Wavelength(nm)	450	550	650	750
Estimated *n*	0.596	1.036	1.512	2.088
Reference *n*	0.618	0.958	1.471	2.402
Error (%) *n*	3.5	8	3	12.5
Estimated *k*	5.20	6.46	7.63	8.40
Reference *k*	5.47	6.69	7.79	8.62
Error (%) *k*	4.9	3.9	2.1	2.55

TABLE 6. Estimated and measured values of surface roughness for the samples at 45°.

Sample	Estimated σ	Measured σ	Error (%)
Aluminium plate	0.392	0.420	6.8
Copper plate	0.346	0.368	6.0

the presented method is applicable to estimate the refractive index from multispectral DOLP measurement, avoiding the measuring errors caused by changing the detection angles from previous methods. Besides, considering the diffuse component of reflection could reduce the impact of the surface state on the parameters estimation. This is helpful for improving accuracy of estimation results for experiments.

We mention that we also validate the effectiveness of presented method at the detection angles from 40° to 60°. However, the experiment results show that, as the detection angle increase, the multispectral DOLP curves only show a slight increase trend, which was consistent with the conclusion from previous works [7], [14]. Besides, the form between different curves is almost similar since the DOLP of aluminum and copper is not sensitive to the detection angle. Therefore, we only present the experiment results of 45° detection angle in this work.

Table 4 lists the estimated results of complex refractive index *n* and *k* for copper plate. We see that the estimated *k* values agrees well with the reference value [29] with errors of about 4%, 9%, 2.4%, 4.1% at 450nm, 550nm, 650nm, 750nm respectively and compared with literature [14] whose error is 8% at 650 nm, the estimated accuracy is improved. The errors of estimated *n* are about 2% at 450nm and 9.5% at 750nm, while the errors at 550 nm and 650 nm are much higher given by about 32% and 22% respectively. However, the deviation of *n* value from reference value at 650nm is slight, given by about 0.05, which do not interfere too much for target recognition. Besides, compared with the results in literature [14] whose deviation is 0.1 from the reference value, the estimate result for *n* is again improved. This improvement may result from that our method takes full advantages of multispectral polarimetric measurements in experiment, which helps to avoid the measurement error caused by changing detection angles. Yang also analyzed the copper plate. However, they cannot estimate the refractive index of copper at 550nm and 650nm because their method is limited by the bound charge of copper. This validates the effectiveness of the presented method to estimate the parameters of metallic surface using multispectral measurements in visible spectral band.

Table 5 lists the estimated results of refractive index for the aluminium plate. We see that the estimated results agree well with the reference value with errors less than 10%, while the

estimation errors for the refraction index of aluminium plate in literature [16] are mostly more than 20%. The improvement in estimation accuracy may be accounted from that the Drude model used in literature [16] is not appropriate for metals when the detection band is near the absorption band of aluminium (about 750nm [30]), while the Lorentz-Drude model we use contains enough harmonic oscillators [32], [33] to describe the dispersion characteristics of metallic materials accurately over the detection band in this paper, which illustrates that the presented method is advantaged to analyze the metallic materials in visible spectral band. Besides, the diffuse component that related to surface roughness in our model may be one of the main reasons why the presented method can estimate the refractive index for rough aluminium plate more accurately than literature [16].

Table 6 lists the values of the estimated σ and measured σ for the samples. We find that the surface roughness can be estimated precisely using the method presented here with errors of 6.8% for aluminium plate and 6.0% for copper plate. The surface roughness is related to the diffuse component of reflection that account for the decrease of the DOLP value of scattered light form target surface. Therefore, taking the surface roughness into account makes the presented method applicable to derive a more accurate DOLP equation for rough targets. In addition the presented method is helpful to obtain the surface characteristic of rough targets.

V. CONCLUSION
In this paper, we present a new method to estimate refractive index and surface roughness of rough metallic targets based on modified DOLP equation, the parameters of interest of targets could be extracted from passive multispectral polarimetric measurements using Levenberg–Marquardt algorithm. The Monte Carlo simulation analyzes the sensitivity of the presented method to the Gaussian noise as well as the number of input measurements. The simulation results suggest that

estimation accuracy improves with the increasing number of input measurements until saturates when the spectral channels reach 21 spectral channels consistent well with the input values in all noisy scenarios. Finally, the experimental results show that the refractive index and surface roughness are estimated accurately with errors for copper mostly given by about 9% and for aluminium mostly less than 5% and the errors of estimated surface roughness for copper is no more than 6% and for aluminium is about 6.8%. This validates the effectiveness of presented method for estimating the parameters of interest of rough metallic targets from multispectral polarization measurements.

Our work takes full advantage of the multispectral polarization measurements in refractive index estimation in purpose of avoiding the measurement error caused by changing detection angles in experiments and the problem of getting wrong information resulted from image shift between multiangle remote sensing images. In addition, taking the diffuse component of reflection into consideration makes the DOLP equation in this paper more appropriate for rough surface. As a result, the estimation accuracy is improved compared with the previous works in literature [14], [16] and the surface characteristic is also obtained through estimation. This is significant for characterizing different materials based on their polarimetric signatures in passive remote sensing application.

This study focuses on recognizing the metallic materials by estimating their parameters of interest from multispectral polarimetric measurements and the measurements are under well-controlled laboratory conditions. Further studies are underway to analyze the model for dielectric materials and broad applications for recognizing manmade rough targets from nature backgrounds in the field environment

REFERENCES

[1] Y. Ding and S. Pau, "Circularly and elliptically polarized light under water and the umov effect," *Light, Sci. Appl.*, vol. 8, no. 1, Dec. 2019, Art. no. 32, doi: 10.1038/s41377-019-0143-0.

[2] H. Zhan, D. G. Voelz, S.-Y. Cho, and X. Xiao, "Complex index of refraction estimation from degree of polarization with diffuse scattering consideration," *Appl. Opt.*, vol. 54, no. 33, pp. 9889–9895, 2015.

[3] J. Yuan, C. Hu, C. Yan, Z. Li, S. Chen, S. Wang, X. Wang, Z. Xu, and X. Ju, "Semi-empirical soil organic matter retrieval model with spectral reflectance," *IEEE Access*, vol. 7, pp. 134164–134172, 2019.

[4] P. Terrier, V. Devlaminck, and J. M. Charbois, "Segmentation of rough surfaces using a polarization imaging system," *J. Opt. Soc. Amer. A, Opt. Image Sci.*, vol. 25, no. 2, pp. 423–430, 2008.

[5] D. Miyazaki, M. Kagesawa, and K. Ikeuchi, "Transparent surface modeling from a pair of polarization images," *IEEE Trans. Pattern Anal. Mach. Intell.*, vol. 26, no. 1, pp. 73–82, Jan. 2004.

[6] X. Zhang, Q. Li, F. Liu, M. Qiu, S. Sun, Q. He, and L. Zhou, "Controlling angular dispersions in optical metasurfaces," *Light, Sci. Appl.*, vol. 9, no. 1, Dec. 2020, Art. no. 76, doi: 10.1038/s41377-020-0313-0.

[7] H. Zhan, H. Jiang, D. G. Voelz, and M. K. Kupinski, "Surface parameter based image estimation from application of a scattering model to polarized light measurements," *Proc. SPIE*, vol. 10407, Aug. 2017, Art. no. 104070U.

[8] F. Goudail, P. Terrier, Y. Takakura, L. Bigué, F. Galland, and V. DeVlaminck, "Target detection with a liquid crystal-based passive Stokes polarimeter," *Appl. Opt.*, vol. 43, no. 2, pp. 274–282, 2004

[9] B. Connor, I. Carrie, R. Craig, and J. Parsons, "Discriminative imaging using a LWIR polarimeter," *Proc. SPIE*, vol. 7113, Oct. 2008, Art. no. 71130K.

[10] F. Cremer, W. de Jong, and K. Schutte, "Infrared polarisation measurements of surface and buried anti-personnel landmines," *Proc SPIE*, vol. 4394, pp. 1–12, Oct. 2001.

[11] J. R. Shell, "Polarimetric remote sensing in the visible to near infrared," Ph.D. dissertation, Rochester Inst. Technol., Rochester, NY, USA, 2005.

[12] S. Tominage and A. Kimachi, "Polarization imaging for material classification," *Opt. Eng.*, vol. 47, no. 12, 2008, Art. no. 123201.

[13] J. Zallat, P. Grabbling, and Y. Takakura, "Using polarimetric imaging for material classification," in *Proc. IEEE Int. Conf. Image Process.*, Sep. 2003, pp. 827–830.

[14] V. Thilak, D. G. Voelz, and C. D. Creusere, "Polarization-based index of refraction and reflection angle estimation for remote sensing applications," *Appl. Opt.*, vol. 46, no. 30, pp. 7527–7536, 2007.

[15] M. W. Hyde, IV, "Determining the complex index of refraction of an unknown object using turbulence-degraded polarimetric imagery," *Opt. Eng.*, vol. 49, no. 12, Dec. 2010, Art. no. 126201.

[16] M. A. Sawyer and M. W. Hyde, IV, "Material characterization using passive multispectral polarimetric imagery," *Proc. SPIE*, vol. 8873, Sep. 2013, Art. no. 88730Y.

[17] B. Yang, C. Yan, J. Zhang, and H. Zhang, "Refractive index and surface roughness estimation using passive multispectral and multiangular polarimetric measurements," *Opt. Commun.*, vol. 381, pp. 336–345, Dec. 2016.

[18] A. D. Rakic, A. B. Djurišic, J. M. Elazar, and M. L. Majewski, "Optical properties of metallic films for vertical-cavity optoelectronic devices," *Appl. Opt.*, vol. 37, no. 22, pp. 5271–5283, Aug. 1998.

[19] A. Vial, A.-S. Grimault, D. Macías, D. Barchiesi, and M. L. de la Chapelle, "Improved analytical fit of gold dispersion: Application to the modeling of extinction spectra with a finite-difference time-domain method," *Phys. Rev. B, Condens. Matter*, vol. 71, no. 8, Feb. 2005, Art. no. 085416.

[20] J. Pan, Q. Chen, W. Qian, and L. Geng, "Results of a new polarimetric BRDF simulation of metallic surfaces," *Infr. Phys. Technol.*, vol. 72, pp. 58–67, Sep. 2015.

[21] R. G. Priest and S. R. Meier, "Polarimetric microfacet scattering theory with applications to absorptive and reflective surfaces," *Opt. Eng.*, vol. 41, pp. 988–993, May 2002.

[22] M. W. Hyde, IV, J. D. Schmidt, and M. J. Havrilla, "A geometrical optics polarimetric bidirectional reflectance distribution function for dielectric and metallic surfaces," *Opt. Express*, vol. 17, no. 24, pp. 22138–22153, 2009.

[23] M. G. Gartley, S. D. Brown, and J. R. Schott, "Micro-scale surface and contaminate modeling for polarimetric signature prediction," *Proc. SPIE*, vol. 6972, Mar. 2008, Art. no. 697213.

[24] H. Zhan, D. G. Voelz, and S.-Y. Cho, "Index of refraction estimation from Stokes parameters with diffuse scattering consideration," *Proc. SPIE*, vol. 9853, May 2016, Art. no. 985304.

[25] ASD. *FieldSpec 4 Standard-Res Spectroradiomcter [EB/OL]*. [Online]. Available: https://www.asdi.com/products-and-services/fieldsperspectroradiometers/ficldspc-4-standard-rcs

[26] T. Marbach, B. Fougnie, A. Lacan, and P. Schlüssel, "Vicarious calibration of the multiviewing channel polarization imager (3MI) of the EUMETSAT Polar System-Second Generation (EPSSG)," *Proc. SPIE*, vol. 10000, Oct. 2016, Art. no. 1000017.

[27] Z. Q. Sun, Z. F. Wu, and Y. S. Zhao, "Semi-automatic laboratory goniospectrometer system for performing multi-angular reflectance and polarization measurements for natural surfaces," *Rev. Sci. Instrum.*, vol. 85, no. 1, Jan. 2014, Art. no. 014503.

[28] F. Cremer, P. B. W. Schwering, W. de Jong, K. Schutte, and A. N. de Jong, "Infrared polarization measurements of targets and backgrounds in a marine environment," *Proc. SPIE*, vol. 4370, pp. 168–180, Sep. 2001.

[29] D. W. Lynch and W. R. Hunter, "Comments on the optical constants of metals and an introduction to the data for several metals," in *Handbook of Optical Constants of Solids*. 1985.

[30] D. Y. Smith, E. Shiles, and M. Inokuti, "The optical properties of metallic aluminum," in *Handbook of Optical Constants of Solids*. 1985.

[31] P. B. Johnson and R. W. Christy, "Optical costants of the noble metals," *Phys. Rev.*, vol. 6, pp. 4370–4379, Dec. 1972.

[32] Y.-C. Chung, P.-J. Cheng, Y.-H. Chou, B.-T. Chou, K.-B. Hong, J.-H. Shih, S.-D. Lin, T.-C. Lu, and T.-R. Lin, "Surface roughness effects on aluminium-based ultraviolet plasmonic nanolasers," *Sci. Rep.*, vol. 7, no. 1, Feb. 2017, Art. no. 39813, doi: 10.1038/srep39813.

[33] X. Fan, W. Zheng, and D. J. Singh, "Light scattering and surface plasmons on small spherical particles," *Light, Sci. Appl.*, vol. 3, no. 6, p. e179, Jun. 2014, doi: 10.1038/lsa.2014.60.

XIN WANG was born in Jilin, Jilin, China, in 1992. He received the B.S. degree in photoelectric information engineering from the Changchun University of Science and Technology, China, in 2015. He is currently pursuing the Ph.D. degree in optical engineering with the Changchun Institute of Optics, Fine Mechanics and Physics, Chinese Academy of Sciences, Changchun, China. His current research interest includes application of polarization spectra.

JING YUAN was born in Changchun, Jilin, China, in 1993. She received the B.S. degree in optical information science and technology from Jilin University, China, in 2016. She is currently pursuing the Ph.D. degree in optical engineering with the Changchun Institute of Optics, Fine Mechanics and Physics, Chinese Academy of Sciences Changchun, China. Her current research interests include application of spectra, hyper-spectral remote sensing, and application of remote sensing in soil.

CHANGXIANG YAN was born in Honghu, Hubei, China, in 1973. He received the M.S. degree in engineering from Zhejiang University, Zhejiang, China, in 1998, and the Ph.D. degree from the Changchun Institute of Optics, Fine Mechanics and Physics, Chinese Academy of Sciences, Changchun, China, in 2001.

Since 2010, he has been the Director of the Space Optics Laboratory, Changchun Institute of Optics, Fine Mechanics and Physics, Chinese Academy of Sciences. His research interests include opto-mechatronics technology for space optical remote sensing instruments, multispectral and hyper-spectral spatial remote sensing imaging, polarization detection, and space surveillance.

YANFENG QIAO was born in Changchun, Jilin, China, in 1962. He received the M.S. degree in engineering from Southeast University, Nanjing, China, in 1985. From 2009 to 2013, he was the Deputy Secretary General of National Technical Committee of Photoelectric Measurement Standardization and the Member of the fifth Aircraft Measurement and Control Committee of Chinese Astronautical Society, from 2004 to 2011. His research interests include optical design for large aperture telescope, autocollimation interference technique for optical measuring, and high-accuracy gyro for direction correction.

JUNQIANG ZHANG was born in Taixing, Jiangsu, China, in 1981. He received the B.S. degree in optical information science and technology from Jilin University, China, in 2007, and the Ph.D. degree in optical engineering from the Changchun Institute of Optics, Fine Mechanics and Physics, Chinese Academy of Sciences, Changchun, China, in 2012. He mainly engaged in polarization, spectral instrument development, optical system performance evaluation, and other aspects of the research.

XUEPING JU was born in Songyuan, Jilin, China, in 1991. He received the B.S. degree in control technology and instruments from Tianjin University, China, in 2014, and the Ph.D. degree in optical engineering from the Changchun Institute of Optics, Fine Mechanics and Physics, Chinese Academy of Sciences, Changchun, China, in 2019. His current research interest includes polarization calibration.

NING DING was born in Shandong, Liaocheng, China, in 1994. She received the B.S. degree in photoelectric information science and engineering from the Harbin Institute of Technology, China, in 2017. She is currently pursuing the Ph.D. degree in optical engineering with the Changchun Institute of Optics, Fine Mechanics and Physics, Chinese Academy of Sciences Changchun, China.

YOUZHI DONG was born in Harbin, Heilongjiang, China, in 1996. He received the B.S. degree in optoelectronic information science and engineering from Jilin University, China, in 2018. He is currently pursuing the M.S. degree in optical engineering with the Changchun Institute of Optics, Fine Mechanics and Physics, Chinese Academy of Sciences Changchun, China. His current research interests include design of optical system of polarization spectral imager and large field of view lens.

• • •